Blend Structure of Commingled Plastic from Recycled Polyethylene and Polystyrene

T. LI,[1] S. HENRY,[2] M. S. SILVERSTEIN,[3] A. HILTNER,[1,*] and E. BAER[1]

[1]Department of Macromolecular Science and Center for Applied Polymer Research, Case Western Reserve University, Cleveland, Ohio 44106; [2]Tremco Inc., Cleveland, Ohio; [3]Department of Materials Engineering, Technion Institute of Technology, Haifa, Israel

SYNOPSIS

The hierarchical morphology of commingled plastic waste in the form of thick beams prepared by the ET-1 process has been examined. Blends of recycled high-density polyethylene (RHDPE, New Jersey Curbside Tailings) with 25 and 35 wt % expanded polystyrene (EPS) were compared with blends of a virgin high-density polyethylene resin (VHDPE). At the macroscale, observed with the optical microscope, the beams consisted of a solid skin that extended about one-third of the distance to the center of the beam and a voided core with about half the density of the skin. The phase morphology of the skin at the microscale was characterized by examining etched cryogenic fracture surfaces in a scanning electron microscope. The blends of RHDPE and VHDPE exhibited a gradient morphology with highly elongated EPS domains near the edge and spherical or co-continuous EPS domains closer to the core. The morphology gradient was created by the competition between the relaxation rate of the melt-flow morphology and the cooling rate in the mold. In addition to high-density polyethylene, a variety of other components were identified in RHDPE by photoacoustic infrared and thermal analysis. These included polypropylene, polystyrene, poly(ethylene terephthalate), and chunks of nonpolymeric material. As a result of the heterogeneous composition, the crystallinity of RHDPE was significantly lower than that of VHDPE.

INTRODUCTION

Plastics can be recycled because thermoplastic resins, which comprise 83% of all plastics and 100% of plastics used in consumer packaging and disposables, can flow upon reheating and thus can be remolded.[1,2] However, only 150–200 million pounds of postconsumer plastics are currently recycled in the United States, which is less than 0.5% of all plastics produced in the United States in 1988 (about 54.5 billion pounds) and less than 1.5% of the plastics used in packaging (13.8 billion pounds).[2] As a result of this seeming lack of activity in plastics recycling, plastics are perceived to be nonrecyclable and environmentally unfriendly. Furthermore, the nondegradable characteristics of plastics ensure their high visibility in landfills and elsewhere.

A major barrier to recycling plastics collected in the postconsumer waste stream is the high cost of separation and cleaning.[3] An alternative approach that has been developed to simplify the procedures and reduce cost is to process the plastic waste stream without complete separation. Specialized equipment such as the Extrusion Technology 1 (ET-1) machine is capable of processing regrinds into plastic lumber and related mixed plastic products.[2]

Components of the plastic waste stream include high- and low-density polyethylene, polypropylene, polyester, polystyrene, and PVC. The major component of mixtures that have been commingled in the ET-1 process is high-density polyethylene (HDPE).[4] As a result, the other components constitute a dispersed phase in a continuous HDPE matrix. It is well known that blending can lead to

* To whom correspondence should be addressed.

Journal of Applied Polymer Science, Vol. 52, 301–314 (1994)
 CCC 0021-8995/94/020301-14

either enhanced or reduced properties. In general, HDPE is not compatible with the other components of the plastic waste stream and synergistic effects are not anticipated. However, even in the case of recycled plastic mixtures, opportunities exist for improving the properties, e.g., by addition of an inexpensive compatibilizer to increase strength and ductility or by addition of a significant quantity of another inexpensive component to increase rigidity. Recently, up to 50 wt % scrap polystyrene has been added to waste plastic mixtures to enhance stiffness.[4]

The properties that are achieved in a commingled plastic mixture are determined to a large extent by the phase morphology and the morphology gradients. Particularly, when plastic waste is commingled in the ET-1 machine, where the composition of the mixture is not known with a high degree of certainty and description of the process variables is complex, it is virtually impossible to predict the phase morphology. For this reason, a detailed characterization was made of the phase morphology in beams produced from plastic waste mixtures by the ET-1 process.

EXPERIMENTAL

Materials

The commingled plastic was provided in the form of beams 2.4 m in length with a square cross section about 66 mm on a side by the Center for Plastics Recycling Research at Rutgers, The State University of New Jersey. The PET soda bottles and unpigmented HDPE milk jars had been removed from unwashed plastic waste collected from several New Jersey communities. The remaining mixture, often referred to as New Jersey Curbside Tailings (NJCT), consisted primarily of HDPE with lesser amounts of numerous other components and is denoted as recycled high-density polyethylene (RHDPE). The RHDPE and a virgin HDPE resin (VHDPE) alone and in mixtures with densified industrial expanded polystyrene scrap (EPS) from Mobile Chemical Co. were extruded from the ET-1 machine into square molds at the Center for Plastics Recycling Research. The compositions included in the study were VHDPE, RHDPE, and blends of VHDPE/EPS 75/25 (wt/wt), RHDPE/EPS 75/25 (wt/wt), and RHDPE/EPS 65/35 (wt/wt). The blends are subsequently referred to as 75VH, 75RH, and 65RH, respectively. Two beams of each composition were provided, one cooled in air and the other in water.

Characterization

A cross-section cut from the center of the beam was polished with progressively finer silicon carbide papers, 320, 800, 1200, and, finally, 2400 grit, and photographed.

For specific gravity measurements, a cylindrical core was drilled along the center line of the cross section near the middle of the beam. The core was cut at approximately 4 mm intervals into eight portions from the edge to the center of the beam. The displacement method, ASTM 792, was used to measure the specific gravity of the portions cut from the solid skin region of the beam. The specific gravity of the porous portions from the voided center of the beam was determined from the weight and the physical dimensions of the portion.

Specimens weighing 2–4 mg were cut from the drilled core portions for differential scanning calorimetry (DSC), Perkin-Elmer Series 7 DSC. Thermal analysis was performed on one specimen from each portion of the VHDPE materials and two specimens of the RHDPE materials. The temperature cycle was heating from 25 to 180°C, cooling to 25°C, and reheating to 400°C, all at 20°C/min. The melting temperature of HDPE and glass transition temperature of polystyrene (PS) were obtained from the initial heating thermogram, and the heats of melting of HDPE and polypropylene were obtained from the second heating thermogram. Indium was used as the calibration standard.

Dynamic mechanical analysis was carried out in the tension mode at 1 and 10 Hz on the DMTA instrument from Polymer Laboratories. Specimens about 1 mm thick, 5 mm wide, and 20 mm in length were cut from the void-free skin region with the length along the mold-filling direction (MFD). Measurements of the real modulus and tan δ were made over the temperature range from −40 to 150°C with a heating rate of 2°C/min.

Photoacoustic Fourier transform infrared (FTIR) analysis was made on specimens cut from the void-free skin region with a diamond blade on a low-speed Isomet saw from Buehler Co. The specimens measured about 1 mm in thickness and 4 × 4 mm in cross section. Infrared measurements were carried out on the Nicolet 800 spectrometer.

Surfaces for scanning electron microscopy (SEM) were prepared by cutting a bar near the middle of the beam and notching it at the center so that the notch was aligned either parallel or perpendicular to the mold-filling direction. The single-edge notched bar, with the notched edge facing down, was clamped on both ends, submerged in liquid nitrogen,

and impacted to cause brittle fracture. The cryogenic fracture surfaces were etched with ethyl acetate for about 40 min to remove the PS. The etched surfaces were coated with 60 Å of gold and observed in the JEOL JSM-35CF SEM.

RESULTS AND DISCUSSION

Macro-morphology

The ET-1 extrusion process typically yielded a beam with numerous voids concentrated in the center of the cross section. The variety in size, number, and distribution of voids among the various compositions is illustrated in Figure 1. The optical micrograph of the beam cross section in Figure 1(a) illustrates the macro-morphology of VHDPE. The cross section was virtually void-free except for a few large voids on the size scale of millimeters near the center. In contrast, the optical micrograph of the 75VH blend [Fig. 1(b)] revealed a distinct "skin–core" macro-morphology. The skin region, which extended approximately one-third of the distance to the center, was essentially void-free. The core region, characterized by a slightly different color, contained nu-

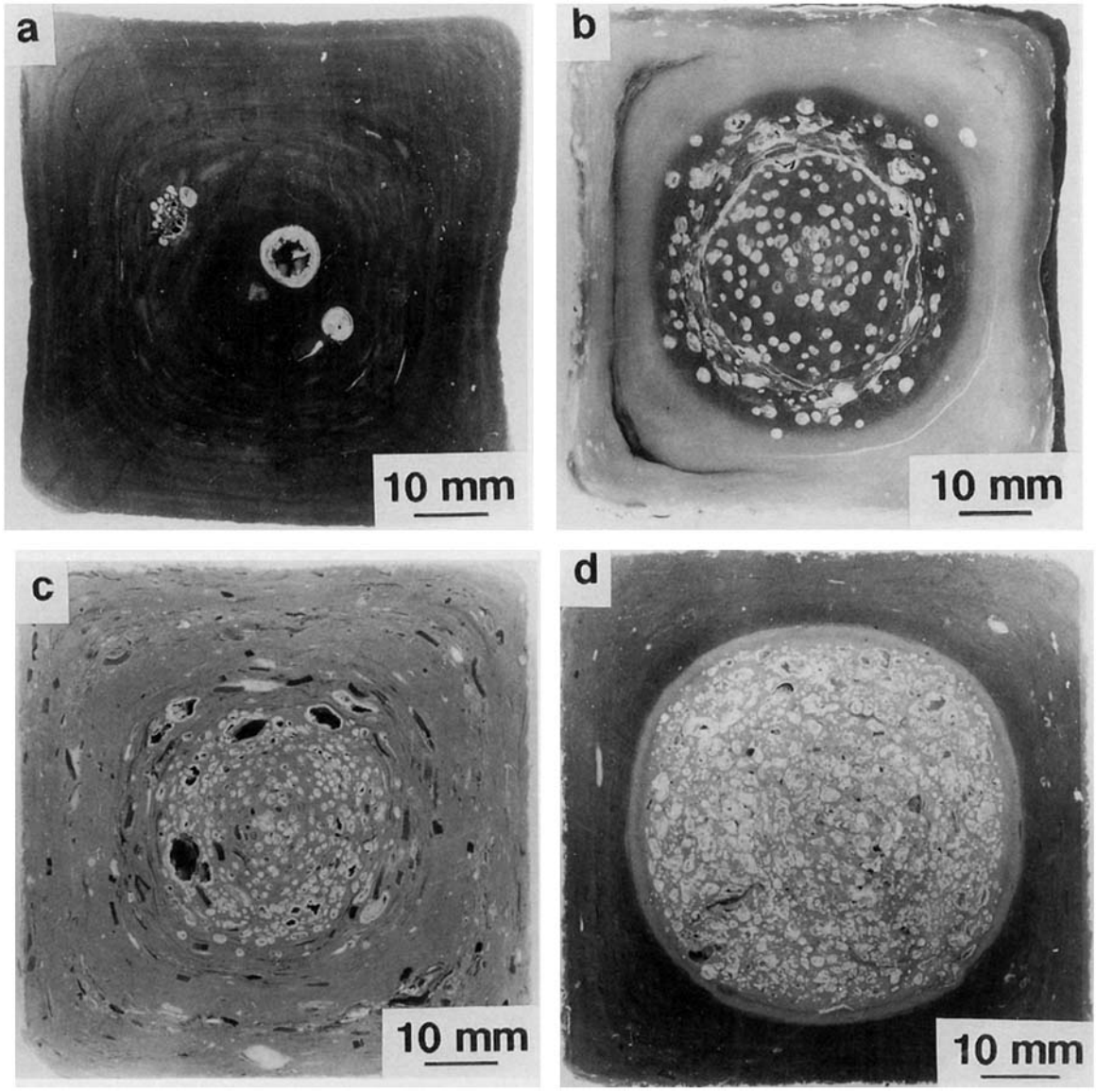

Figure 1 Cross sections of commingled plastic beams (air-cooled): (a) VHDPE; (b) 75VH; (c) RHDPE; (d) 75RH.

merous millimeter-sized voids. Both skin and core featured some concentric splitting or delamination lines that were created by the flow field during processing.

The skin–core macro-morphology was also clear in the beams molded from RHDPE and RHDPE blends [Fig. 1(c) and (d)]. The distinctness of the boundary between the skin and core was emphasized by the somewhat different colors of the skin and core. Unlike the VHDPE blend, RHDPE and RHDPE blends did not exhibit the flow-induced concentric splitting. The cooling rate had no significant effect on the skin–core macro-morphology. The skin of the water-cooled beams solidified more rapidly than did the air-cooled beams; as a result, the edges of the former were relatively flat while the edges of the air-cooled beams were slightly concave to the extent that the cross section was about 3 mm smaller in the center.

The RHDPE contained a significant amount of incompatible material that was distinguishable in the optical micrographs as colored chunks or pieces. Metal chips were one of the other components in RHDPE. Identification of the nonpolyethylene organic components was possible from the photoacoustic infrared spectra in Figure 2. Various bands were observed in the spectrum of RHDPE that were not present in the spectrum of VHDPE. These included the polypropylene (PP) band at 1370 cm^{-1} and a polystyrene (PS) band at 757 cm^{-1}. In addition, characteristic bands for poly(ethylene terephthalate) (PET) were prominent at 1015, 1100, 1220, and 1720 cm^{-1}.[5,6] Because of its high melting temperature, the PET did not melt during processing and was present as particulate material in RHDPE and RHDPE blends. In addition to PET, PS, and PP, RHDPE could also have contained some low-density polyethylene (LDPE) and PVC. The presence of these could not be confirmed by infrared because the bands of HDPE and LDPE overlap and a PET band overlaps the characteristic PVC band at 1740 cm^{-1}.[7]

The density profiles corresponding to two of the cross sections in Figure 1, 75VH and 75RH, are shown in Figure 3. The density profile through the thickness provided an average measure of the amount of voiding and also served to characterize the boundary between the skin and core. The sharp drop in density of the RHDPE blend about 10 mm from the edge coincided with the position of the very distinct skin–core boundary (arrow). The VHDPE blend had a more gradual decrease in density, be-

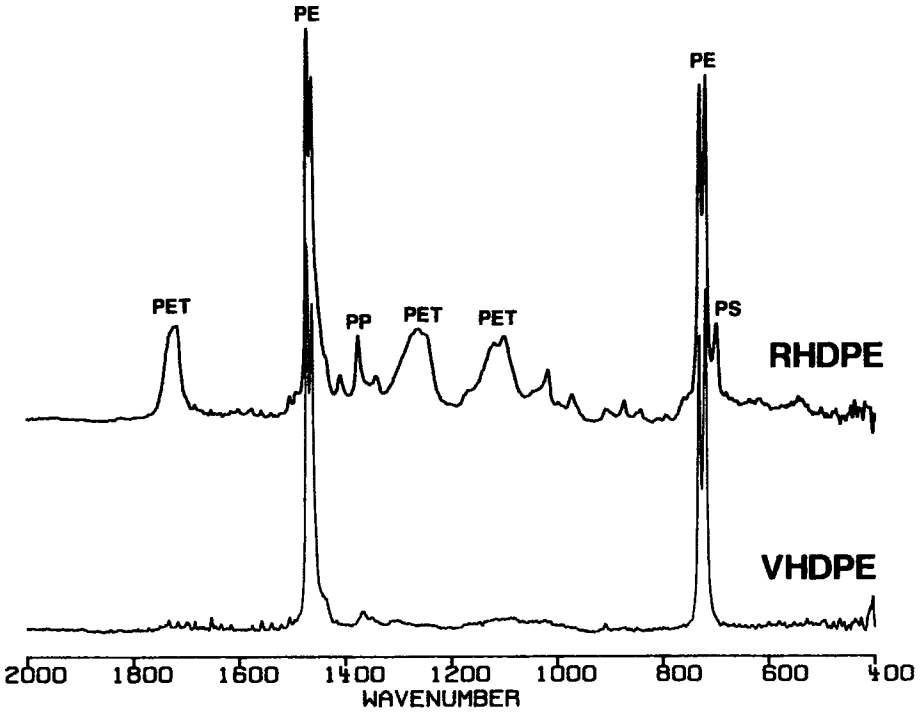

Figure 2 Photoacoustic infrared spectra of VHDPE and RHDPE (air-cooled).

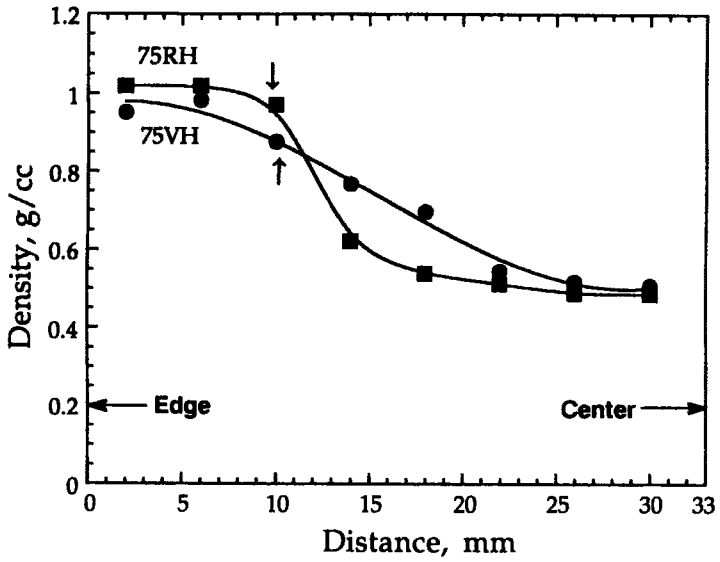

Figure 3 Density through the thickness of commingled plastic beams of 75RH and 75VH (air-cooled). The arrows indicate the position of the skin–core interface.

ginning about 6 mm from the edge. This correlated well with the less distinct skin–core boundary in the optical micrograph.

Most of the other components in RHDPE had a higher density than that of HDPE as indicated by the higher skin density of RHDPE (1.00 g/cc) compared to VHDPE (0.96 g/cc); likewise, the skin density of the 75RH (1.02 g/cc) was higher than that of 75VH (0.97 g/cc). The cooling rate had no discernible effect on the density of the skin or the density profile through the thickness.

Voids reduced the density of the core to about half that of the skin. Differential shrinkage could account for only 3–6 vol % based on the linear expansion coefficient of HDPE.[8] Other causes of voiding included residual foaming agent in the densified expanded polystyrene (EPS), moisture and solvent in the feed stocks, and air entrapped in the short barrel extruder of the ET-1 machine.

Thermal Properties

The most distinct feature of the thermograms of VHDPE and RHDPE was the melting peak at about 135°C. The heat of melting calculated from the area under the melting endotherm did not vary through the thickness of either VHDPE or RHDPE beams. The average heat of melting was 178 J/g for VHDPE and 126 J/g for RHDPE. Assuming that the HDPE crystallized to the same extent in both VHDPE and RHDPE, the RHDPE was estimated to be only 71% HDPE from the difference between the heats of melting of VHDPE and RHDPE. Although it is generally observed that the crystallinity of polyolefins decreases somewhat when they are blended with PS,[9] the reported decreases are not large enough to account for the difference in the heat of melting of VHDPE and RHDPE. The thermal analysis results were attributed to the presence of significant amounts of other polymers in RHDPE.

At least two of the other components of RHDPE were detectable in the thermogram. A small endotherm at 160°C with a heat of melting of about 3 J/g suggested the presence of PP, and the inflection at 105°C was identified as the glass transition of PS. The absence of a detectable inflection at the glass transition temperature of PVC, or any indication of a LDPE melting peak, suggested that these polymers, if present at all, were only in small amounts. The presence of PET was clearly indicated by the FTIR but the melting endotherm was not observed in the thermogram. Since the processing temperature of the ET-1 machine, about 220°C, was not high enough to melt and disperse the PET, this component was present as millimeter-sized flakes. When one of these flakes was physically separated and submitted to thermal analysis, a large melting endotherm at about 250°C identified it as PET.

The melting temperature of HDPE was 3–4°C lower in the blends of VHDPE and RHDPE. In general, there was no significant difference in the thermograms from the skin and core, nor was there any

Table I Thermal Properties of VHDPE, RHDPE, and Their Blends with EPS

Material	Cooling	T_m (°C) (±1–3°)	ΔH_m (J/g) (±2–5°)	Wt % HDPE from VHDPE	Expected Wt % HDPE from RH
VH	Water	135	178	—	—
75VH	Water	131	138	78	—
75VH	Air	133	138	78	—
RH	Water	134	126	71	—
75RH	Water	131	103	58	53
75RH	Air	130	104	58	53
65RH	Water	131	90	51	46
65RH	Air	133	91 ± 11	51	46

significant difference between air-cooled and water-cooled beams. The weight percent of HDPE in the blends was estimated from the ratio of the heat of melting in the blend to the heat of melting of VHDPE. The compositions are summarized in Table I. Because of other components in the RHDPE, the compositions of 75VH and 75RH blends were very different, and 75VH actually had a higher HDPE heat of melting than RHDPE. When the blend composition obtained from the heat of melting was compared with the composition of the feed, the correlation was found to be very good: 75VH was calculated to be 78% HDPE compared to nominally 75% in the feed, and 75RH and 65RH were calculated to be 58% and 51% HDPE, respectively, compared to nominally 53% and 46%, respectively, assuming that RH was 71% HDPE.

The real modulus and tan δ over the temperature

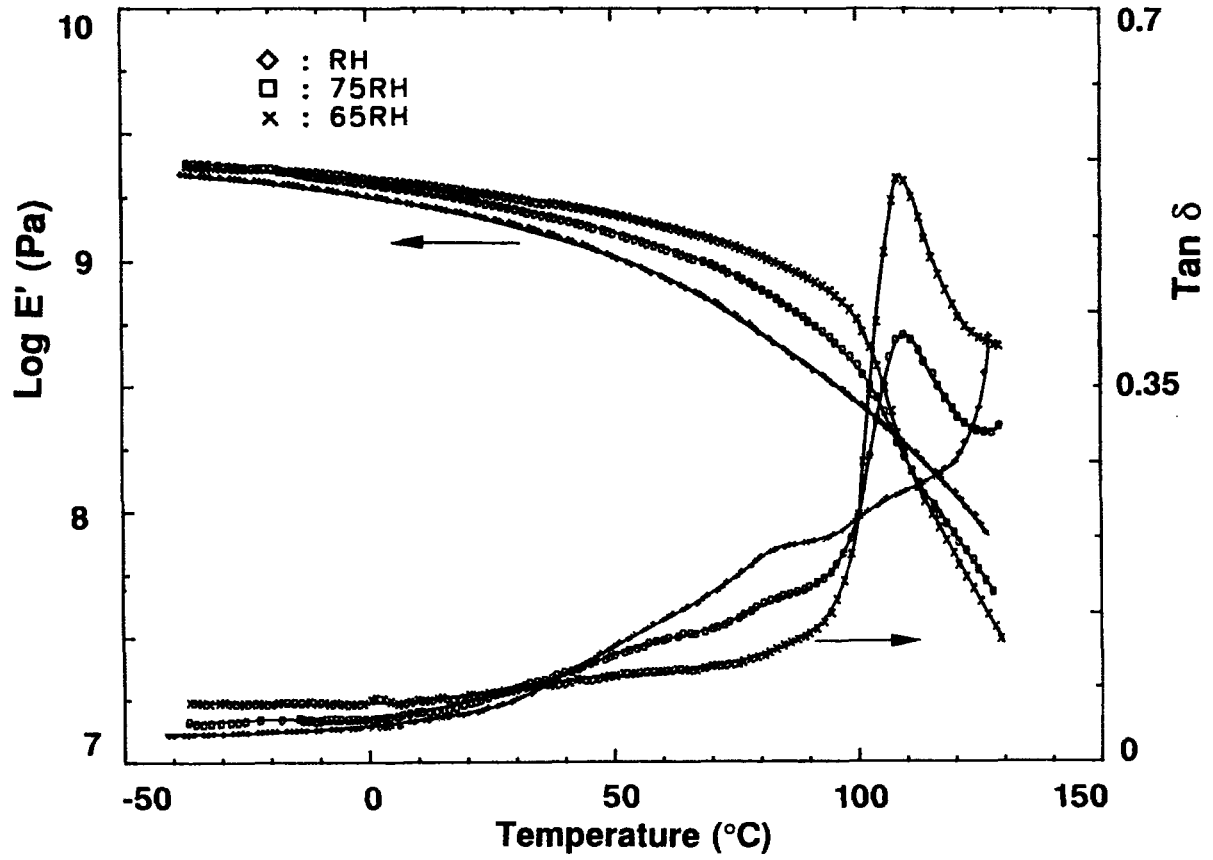

Figure 4 Dynamic mechanical loss curves of RH, 75RH, and 65RH (water-cooled).

range from −40 to 130°C are plotted in Figure 4 for RHDPE and its blends. Between 50 and 100°C, the damping decreased as the amount of EPS increased. This temperature region contains the characteristic α and α' damping peaks of HDPE,[10,11] and the decrease in intensity was consistent with the decreasing amount of RHDPE. The distinct peak at 108°C in the loss curve of 75RH identified the primary transition of EPS since the maximum tan δ value increased when the percentage of EPS in the blend increased from 25 to 35%. The glass transitions of at least two of the other components of RHDPE, PET and PS, were near 110°C and contributed to the broad damping in this temperature range.

Micro-morphology of 75VH

The sequence of low-magnification micrographs in Figure 5 shows the entire cross section of the skin of 75VH. The magnification of 20× was too low for the phase morphology to be clearly discerned. However, two types of morphological textures were distinguishable at this scale, which was termed the mesoscale since it was intermediate between macroscale and microscale. Most of the thickness contained large, musclelike domains on the size scale of 0.5–2.0 mm. Only a region that penetrated about 1.5 mm inward from the edge exhibited a relatively fine texture where these large domains were absent.

Two higher magnification views of the musclelike domains, one from an unetched fracture surface and the other from a fracture surface after it was etched to remove the EPS phase, are compared in Figure 6. A musclelike domain was easily discerned on the unetched surface [Fig. 6(a)] because the specimen fractured along the interface between domains. This micrograph also showed the phase morphology within the musclelike domains to consist of more or less spherical EPS particles dispersed in the PE matrix. The adhesion between the phases did not appear to be very good; the combination of spherical EPS particles protruding from the surface and circular holes that had contained EPS particles indicated that fracture occurred at the interface.

The distribution of the EPS phase was characterized further by comparing the unetched fracture surface in Figure 6(a) with another fracture surface in Figure 6(b) that had been etched to remove the EPS phase. Figure 6(b) shows that large crevices separated the musclelike domains, whereas in Figure 6(a), the domains abutted one another. This suggested that there was a continuous or semicontinuous EPS phase that enveloped and defined the musclelike domains. In addition, the circular holes

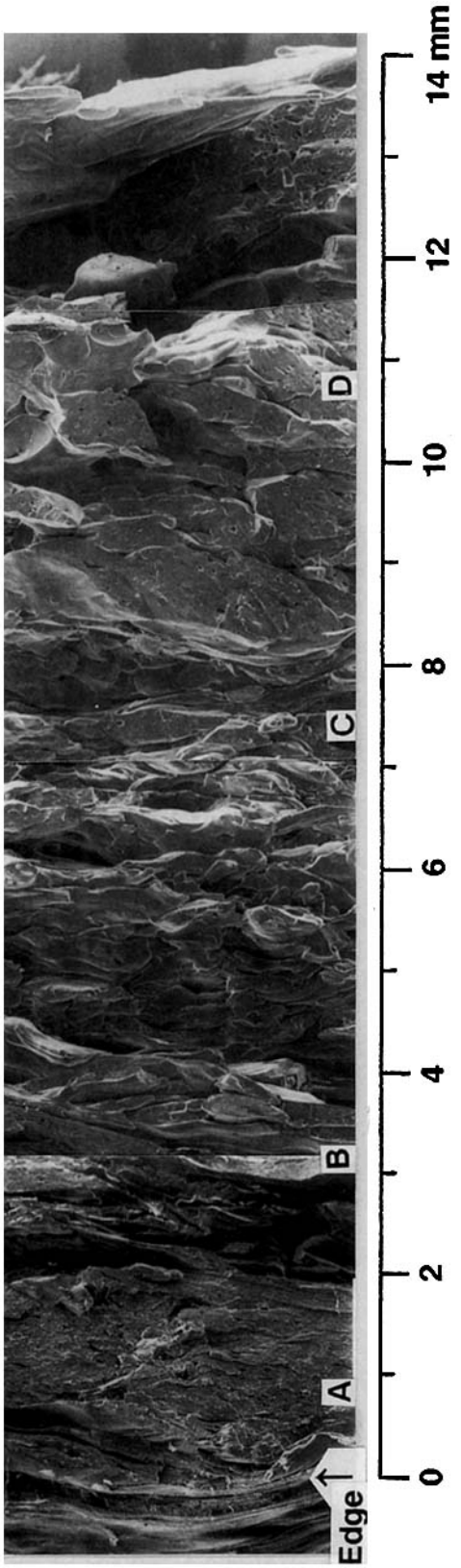

Figure 5 A collage of low-magnification (20×) SEM micrographs through the thickness of 75VH (air-cooled) in the parallel orientation.

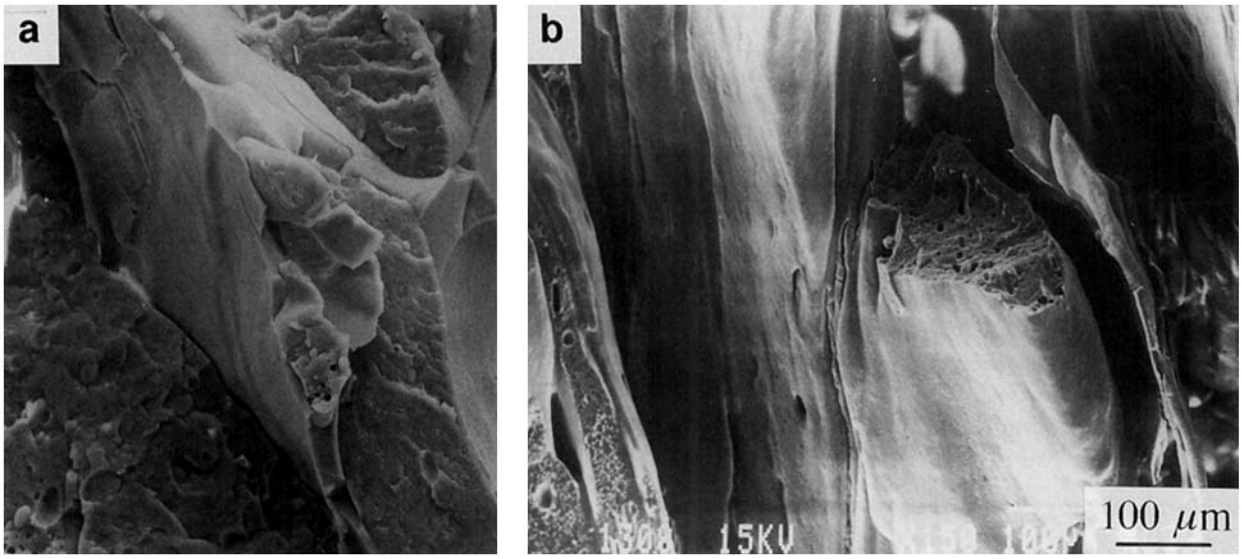

Figure 6 SEM micrographs (150×) of 75VH (air-cooled) in the parallel orientation: (a) unetched; (b) etched.

that remained within the musclelike domain after etching were confirmation that EPS was also dispersed as spherical particles within the PE that formed the matrix of the musclelike domains.

Details of the dispersed EPS phase morphology in the skin were revealed by examination of etched specimens that had been cryogenically fractured both perpendicular and parallel to the mold-filling direction. The positions of the etched cryogenic fracture surfaces are identified in the schematic drawing of the commingled beam in Figure 7. The morphology gradient through the thickness of the skin is shown in Figure 8, a series of micrographs obtained at the four positions identified as positions A–D. The region close to the edge at position A, where there was no musclelike mesoscale structure, contained thin, elongated EPS domains oriented in the mold-filling direction. The EPS domains exhibited considerable variation in both length and width. The length of the domains, determined from the parallel view, was typically in the range of 20–200 μm, although sometimes it was much longer. The cross-sectional shape of the elongated domains was revealed in the perpendicular view. The circular holes 1–5 μm in diameter were indicative of rod-shaped domains, whereas the elongated cross-sections suggested ribbonlike shapes.

The three other positions at which the dispersed EPS phase morphology was examined were in the part of the cross section that had the musclelike domains, positions B–D in Figure 8. The parallel view at position B showed that the EPS domains were thicker and less elongated than at position A. From the circular holes in the perpendicular view, it was apparent that the EPS domains were primarily rod-shaped and about 5–10 μm in diameter. Further from the edge, at position C, the anisotropic shape of the EPS domains almost disappeared. The domains in this region had the shape of large ellip-

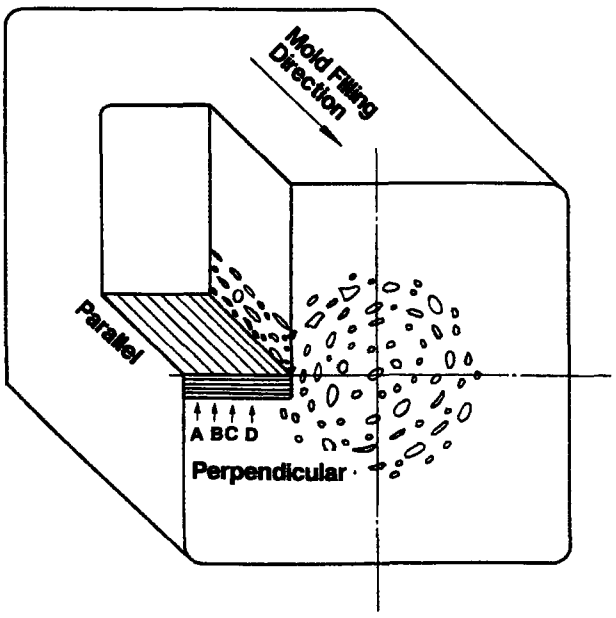

Figure 7 Schematic diagram indicating the positions and orientations at which the micro-morphology of the skin was characterized.

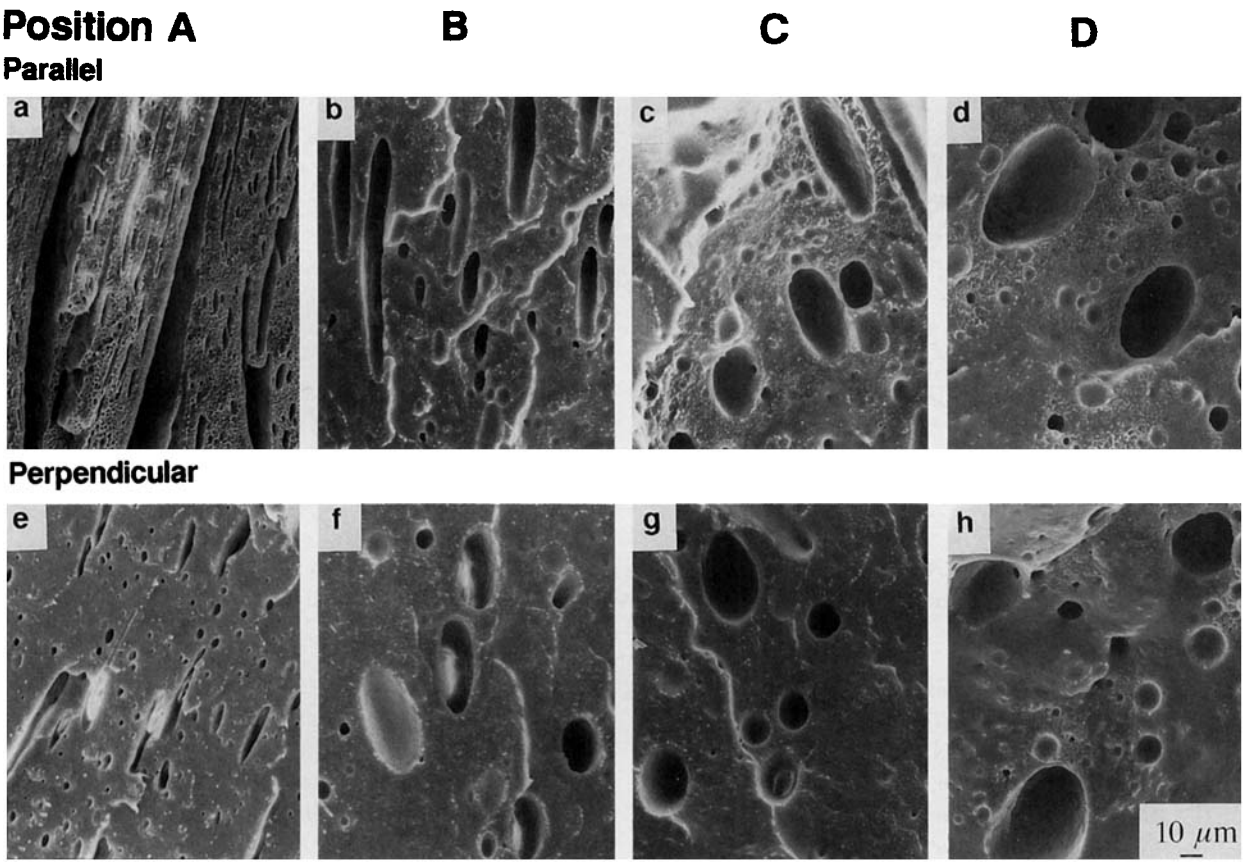

Figure 8 SEM micrographs (500×) of 75VH (air-cooled) at various positions through the thickness of the skin: (a–d) parallel orientation at positions A–D; (e–h) perpendicular orientation at positions A–D.

soids with a wide range of sizes but typically about 50 μm in length and 20 μm in diameter. There was very little further change in the shape of the EPS domains at position D, only a slight increase in the size of the ellipsoidal domains.

A model of the gradient morphology through the thickness of the skin was developed from the micrographs (Fig. 9). A mesostructure that consisted of musclelike domains on the size scale of 0.5–2.0 mm was observed through the thickness of the skin except in a region that extended inward from the edge about 1.5 mm [Fig. 9(a)]. The mesoscale domains were separated and defined by a continuous or semicontinuous EPS phase. Within the musclelike domains, the continuous phase was PE. The portion of the EPS that was not in the interdomain regions of the mesostructure was dispersed as smaller descrete domains in the PE. The size and shape of the dispersed EPS domains are shown schematically in Figure 9(b). In the region that extended about 2 mm inward from the edge and did not exhibit a larger-scale mesostructure, EPS was dispersed in the PE matrix as thin ribbons that were oriented parallel to the edge. Typical dimensions of the ribbons were 90 μm in length, 50 μm in width, and 5 μm in thickness. Interspersed among the ribbons, there were also EPS domains with rodlike, ellipsoidal, and spherical shapes. Toward the center, the EPS domains gradually became thicker and shorter. In the region from about the midpoint of the skin to the core, the EPS domains had the shape of large ellipsoids.

Micro-morphology of 75RH

The unetched fracture surfaces of RHDPE were featureless with no discernible domain morphology. After etching with ethyl acetate, a number of small holes were visible on the fracture surface. These probably indicated the presence of PS domains since the other polymers that were thought to be present in RHDPE, such as PP, LDPE, PVC, and PET, were not dissolved by the etchant, ethyl acetate, at room temperature.

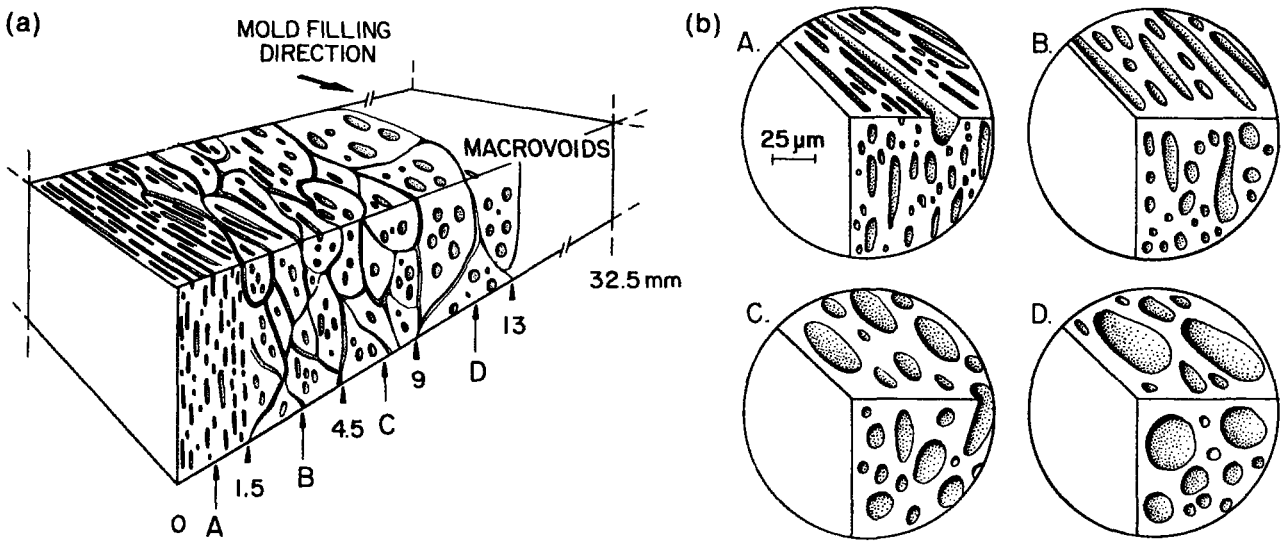

Figure 9 Schematic illustration of the hierarchical morphology of the skin in 75VH (air-cooled): (a) morphology gradient through the thickness; (b) EPS domain morphology.

The skin region of RHDPE blends did not exhibit a morphological texture at the mesoscale analogous to the musclelike domains that were characteristic of 75VH. At the microscale, the morphology gradient of the dispersed EPS phase through the skin was revealed in specimens that had been cryogenically fractured both perpendicular and parallel to the mold-filling direction and etched with ethyl acetate (Fig. 10). Close to the edge, at position A, the elongated EPS domains ranged in length from less than 10 μm to 200 μm, and typically were 10 μm or less in thickness. The shape of the cross sections in the perpendicular view indicated that the elongated domains were narrow ribbons or rods. Frequently, small subinclusions remained in the holes where the EPS had been etched away. At position B, about 2–3 mm from the edge, the EPS domains were thinner and more elongated than at position A, and the cross sections were circular. Rod-shaped domains about 5 μm in diameter and up to 200 μm in length were observed in this region of the skin.

The most significant change in the morphology occurred further from the edge, between positions B and C. Whereas the EPS domains at position B were characterized by a high aspect ratio, at position C, they were thicker and much less elongated. A comparison of the parallel and perpendicular views indicated that some of the domains were almost spherical at position C. Further changes in the morphology between positions C and D were subtle: The etched domains were somewhat larger at position D, which gave the morphology a coarser appearance. As the domains became less elongated, the diameter of the largest domains increased from about 20 μm at position C to 40 μm at position D. At all positions, most of the cavities left by the dissolved EPS contained subinclusion particles 5–10 μm in diameter.

Injection-molded pieces typically retain a morphology gradient since the phase morphology created by the complex flow field during mold filling relaxes to a varying extent before solidification. The morphology gradient through the thickness of the skin is created by the competition between the relaxation rate and the cooling rate after mold filling. The model in Figure 11(a) of the gradient morphology through the thickness of the skin of 75RH was developed from the micrographs. The morphology close to the edge, where the cooling was fastest, most closely resembled the melt morphology during mold filling. The EPS domains were elongated ribbon shapes that became longer and thinner a short distance, about 1 mm, inward from the edge. This was somewhat different from 75VH where the EPS domains were the most highly extended at the edge and gradually became less extended away from the edge. Further from the edge, the slower cooling rate after mold filling favored relaxation of the elongated EPS domains, and beginning about half the distance through the skin, the domain morphology of 75RH was distinctly coarser and less anisotropic than at the edge.

Overall, the EPS domains were distinctly smaller in 75RH than in 75VH. Material properties of the components, such as interfacial tension and rheological characteristics, have a major effect on size and shape of domains. Rheological differences be-

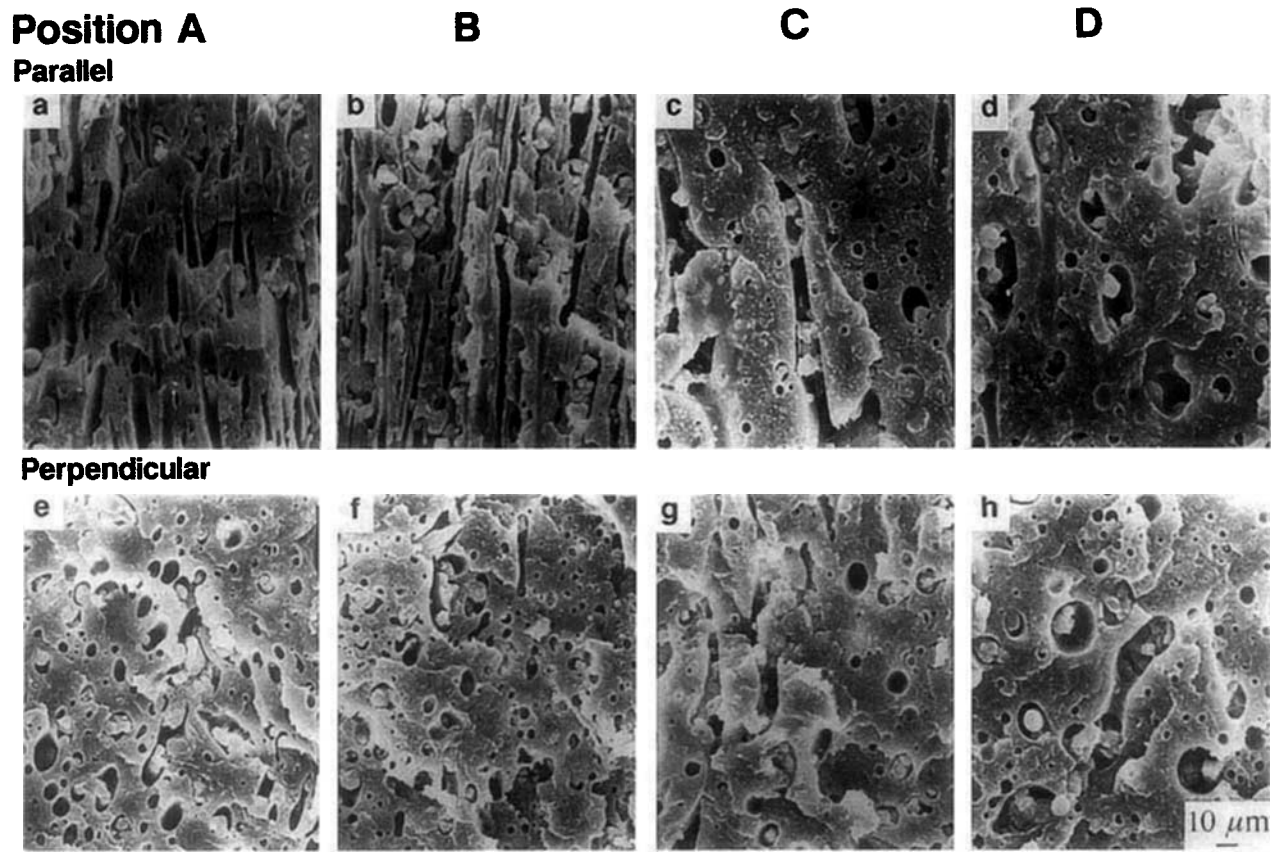

Figure 10 SEM micrographs (500×) of 75RH (air-cooled) at various positions through the thickness of the skin: (a–d) parallel orientation at positions A–D; (e–h) perpendicular orientation at positions A–D.

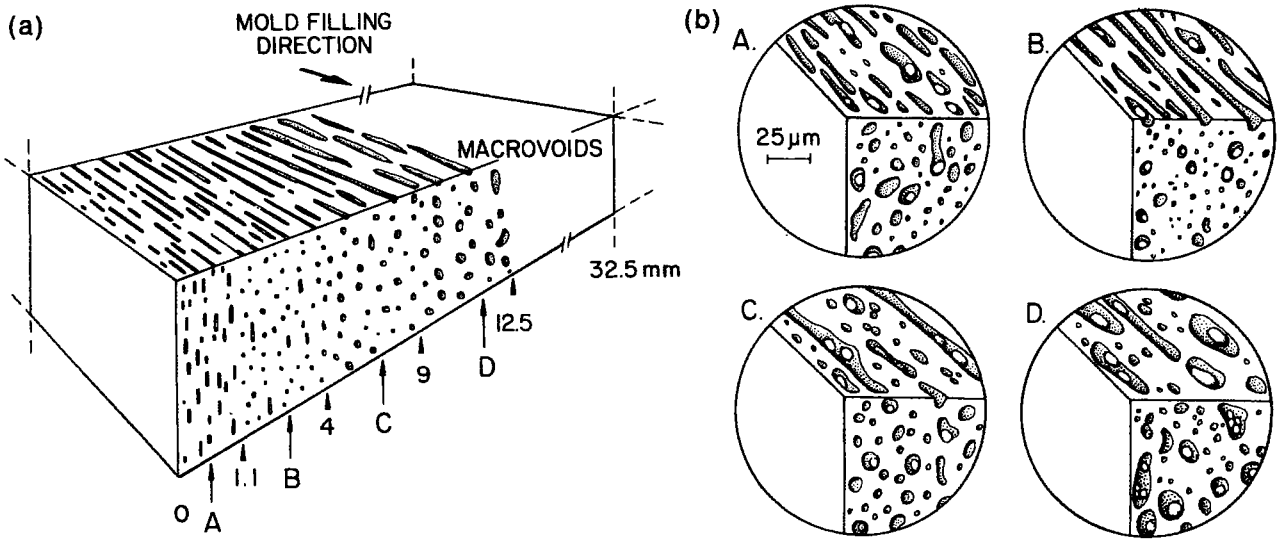

Figure 11 Schematic illustration of the hierarchical morphology of the skin in 75RH (air-cooled): (a) morphology gradient through the thickness; (b) EPS domain morphology.

tween RHDPE and VHDPE might have been partially responsible for differences in the morphology of their blends with EPS. The other components of RHDPE might have altered the rheological properties of the melt or, alternatively, might have affected the interfacial tension in the same way that a compatibilizer would.

Small subinclusions remained in the holes after the EPS was etched away from 75RH [Fig. 11(b)]. Further from the edge, where the EPS domains had relaxed and coarsened, a single hole might contain 10–20 of these particles. Various etchants were used in an attempt to identify this component, which appeared to be immiscible with either EPS or HDPE. The particles were impervious to THF, a solvent for PVC, and to isooctane at 75°C, a condition for dissolving LDPE. When a selective solvent for the particles could not be found, the 75RH was exhaustively extracted with ethyl acetate for 30 h at ambient and the etching solution was centrifuged to separate the suspended particles from the dissolved EPS. Subsequent DSC analysis of the centrifugate identified the particles as being predominantly HDPE. Since RHDPE was a mixture of plastics, it was likely to contain HDPE resins that were not completely miscible.

Micro-morphology of 65RH

The skin morphology of the RHDPE blend with a larger EPS content is shown in the etched cryogenic fracture surfaces in Figure 12. The holes that remained after etching revealed that the EPS domains of 65RH were highly elongated ribbons near the edge, positions A and B. Coalescence of the EPS domains into a layered morphology was suggested by the parallel and perpendicular views. At position C, where the melt had relaxed to a larger extent before solidifying, the layered morphology was not as well defined and the EPS domains appeared to be more interconnected. The melt had the longest time to relax during cooling at position D. Here, about 11 mm from the edge, the domain morphology was coarse, co-continuous, and essentially isotropic.

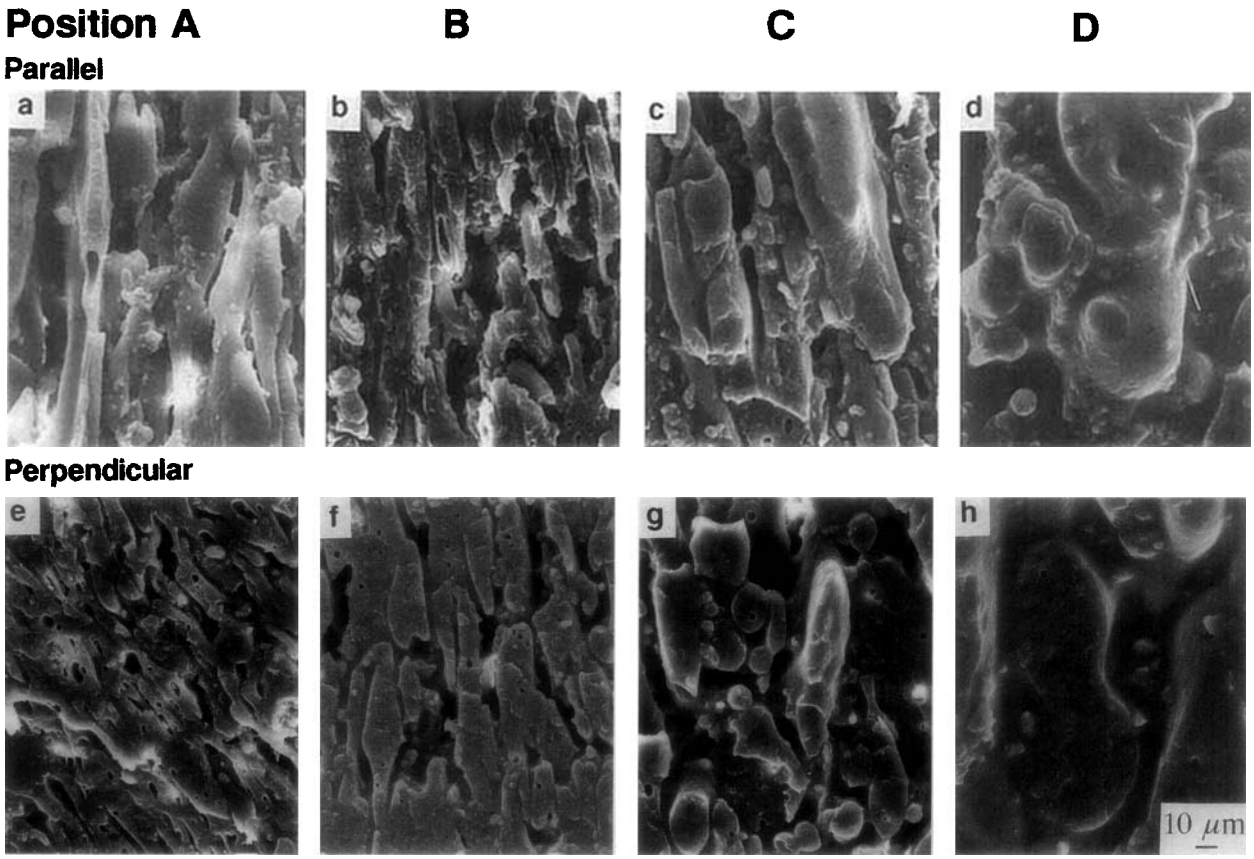

Figure 12 SEM micrographs (500×) of 65RH (air-cooled) at various positions through the thickness of the skin: (a–d) parallel orientation at positions A–D; (e–h) perpendicular orientation at positions A–D.

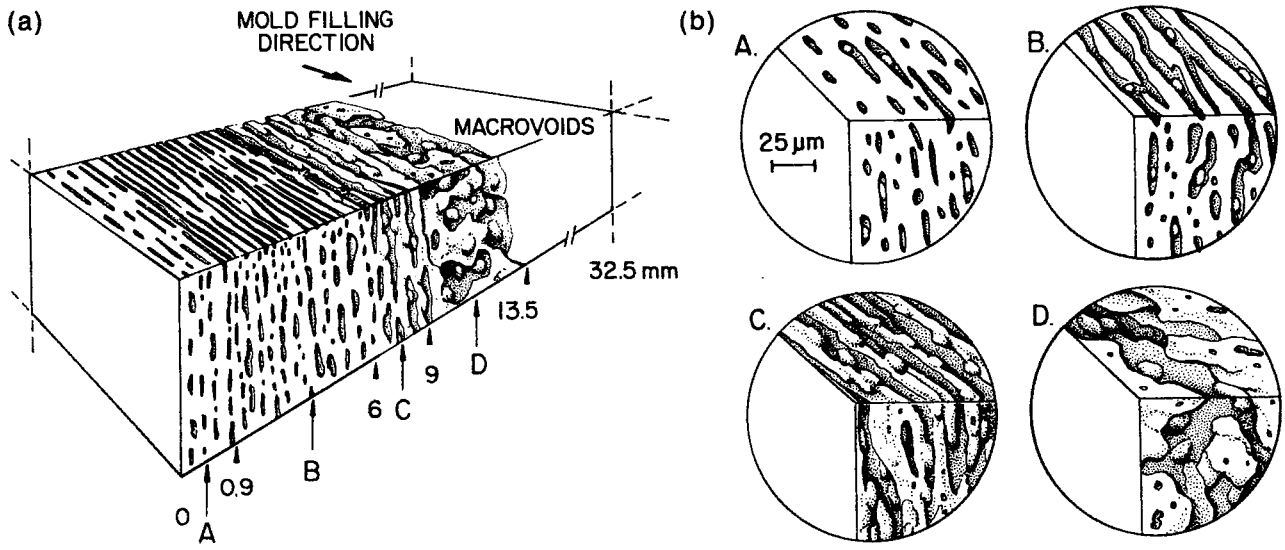

Figure 13 Schematic illustration of the hierarchical morphology of the skin in 65RH (air-cooled): (a) morphology gradient through the thickness; (b) EPS domain morphology.

Many HDPE subinclusion particles remained on all the surfaces after etching.

A model of the gradient morphology through the thickness of the skin of 65RH was developed from the micrographs (Fig. 13). The ribbon-shaped EPS domains close to the edge, where the melt cooled the fastest, were wider and thicker than in 75RH. The EPS ribbons were wide enough to give the morphology a layered appearance in this region. Further from the edge, relaxation of the elongated EPS domains resulted in gradual coarsening of the morphology. In the region furthest from the edge and closest to the voided core, the EPS phase had coalesced into large domains that were co-continuous with the RHDPE phase.

CONCLUSIONS

Thick beams of recycled high-density polyethylene (RHDPE) or virgin high-density polyethylene (VHDPE) blended with expanded polystyrene (EPS) were molded by the ET-1 process. Characterization of the phase morphology led to the following conclusions:

1. At the macroscale, the molded beams consisted of a solid skin that extended about one-third of the distance to the center of the beam and a voided core with about half the density of the skin.
2. In the 75VH blend, the skin possessed a mesoscale structure, consisting of musclelike domains 0.5–2.0 mm in size separated by a continuous or semicontinuous EPS phase, that was absent in the 75RH and 65RH blends.
3. As a result of the competition between the relaxation rate of the melt-flow morphology and the cooling rate in the mold, the blends exhibited a gradient morphology at the microscale with highly elongated EPS domains near the edge and almost spherical or co-continuous EPS domains closer to the core.
4. In addition to high-density polyethylene (HDPE), a variety of other components were identified in RHDPE, including polypropylene, polystyrene, and chunks of nonmelting material such as metal and PET, that were responsible for the lower crystallinity of RHDPE compared to VHDPE.

The authors thank Mr. Ted Kasternakis and Dr. Thomas J. Nosker of the Center for Plastics Recycling Research for providing the samples. This research was jointly sponsored by the National Science Foundation (EEC 81-16103) and the Edison Polymer Innovation Corp. (EPIC).

REFERENCES

1. M. M. Nir, *Plast. Eng.*, **46**(9), 29 (1990).
2. Editorial, *Mod. Plast.*, **66**(9), 43 (1989).

3. D. Spencer, *Waste Solutions* (a supplement to *Mod. Plast.*), **67**(4), 19 (1990).
4. K. E. Van Ness and T. J. Nosker, in *Plastics Recycling*, R. J. Ehrig, Ed., Hanser Verlag, Munich, 1992, Chap. 9.
5. M. M. Coleman and P. C. Painter, in *Encyclopedia of Polymer Science and Engineering*, Vol. 8, H. M. Mark, N. M. Bikales, C. G. Overberger, G. Menges, and J. I. Kroschwitz, Eds., Wiley, New York, 1987, pp. 79–84.
6. D. S. Dunn and A. J. Ouderkirk, *Macromolecules*, **23**, 770 (1990).
7. K. Volka, J. Škorvaga, and Z. Vymazal, *Spectrochimica*, **44A**, 1341 (1988).
8. *Mod. Plast. Encycl.*, **62**(11), 409 (1992).
9. A. Aref-Azar, J. N. Hay, B. J. Marsden, and N. Walker, *J. Polym. Sci. Polym. Phys. Ed.*, **18**, 637 (1980).
10. R. F. Boyer, in *Encyclopedia of Polymer Science and Technology*, supplement Vol. 2, H. M. Mark and N. M. Bikales, Eds., Interscience, New York, 1977, pp. 745–839.
11. I. M. Ward, *Mechanical Properties of Solid Polymers*, 2nd ed., Wiley, New York, 1983, pp. 177–193.

Received August 3, 1993
Accepted September 5, 1993